Received: 23 December 2022 | Revised: 1 May 2023 | Accepted: 8 May 2023

DOI: 10.1111/bcpt.13918

ORIGINAL ARTICLE

BCPT Basic & Clinical Pharmacology & Toxicology

Adverse effects of an aldosterone synthase (CYP11B2) inhibitor, fadrozole (FAD286), on inflamed rat colon

Hanna Launonen[1] | **Lotta Luiskari**[1] | **Jere Linden**[2] | **Aino Siltari**[1,3] | **Hanne Salmenkari**[4,5,6] | **Riitta Korpela**[1,7] | **Heikki Vapaatalo**[1]

[1]Faculty of Medicine, Pharmacology, University of Helsinki, Helsinki, Finland

[2]Faculty of Veterinary Medicine, Department of Veterinary Biosciences and Finnish Centre for Laboratory Animal Pathology (FCLAP), HiLIFE, University of Helsinki, Helsinki, Finland

[3]Faculty of Medicine and Health Technology, Tampere University, Tampere, Finland

[4]Folkhälsan Research Center, Folkhälsan Institute of Genetics, Helsinki, Finland

[5]Abdominal Center, Nephrology, University of Helsinki and Helsinki University Hospital, Helsinki, Finland

[6]Research Program for Clinical and Molecular Metabolism, Faculty of Medicine, University of Helsinki, Helsinki, Finland

[7]Faculty of Medicine, Human Microbiome Research Program, University of Helsinki, Helsinki, Finland

Correspondence
Hanna Launonen, Faculty of Medicine, Pharmacology, University of Helsinki, PO. Box 63, 00014 University of Helsinki, Helsinki, Finland.
Email: hanna.launonen@helsinki.fi

Funding information
Finska Läkaresällskapet; Mary and Georg C. Ehrnrooth's Foundation; Maud Kuistila Memory Foundation; Paulo Foundation; Finnish Cultural Foundation (Kymenlaakso regional fund, Olavi and Alli Pietikäinen fund)

Abstract

Recently, we described local aldosterone production in the murine large intestine. Upregulated local aldosterone synthesis in different tissues has been linked with inflammatory conditions, which have been attenuated by the aldosterone synthase (CYP11B2) inhibitor, fadrozole (FAD286). Therefore, we investigated the effect of inhibition of intestinal aldosterone synthesis on the development of intestinal inflammation. Sprague-Dawley rats were administered 5% (v/w) dextran sodium sulphate (DSS) for 7 days with or without daily FAD286 (30 mg/kg/d) subcutaneous injections on 3 days before, during and one day after DSS. Tissue aldosterone concentrations were evaluated by ELISA, CYP11B2 by Western blot and RT-qPCR. FAD286 halved adrenal aldosterone production but, intriguingly, increased the colonic aldosterone concentration. The lack of inhibitory effect of FAD286 in the colon might have been affected by the smaller size of colonic vs. adrenal CYP11B2, as seen in Western blot. When combined with DSS, FAD286 aggravated the macroscopic and histological signs of intestinal inflammation, lowered the animals' body weight gain and increased the incidence of gastrointestinal bleeding and the permeability to iohexol in comparison to DSS-animals. To conclude, FAD286 exerted harmful effects during intestinal inflammation. Local intestinal aldosterone did not seem to play any role in the inflammatory pathogenesis occurring in the intestine.

KEYWORDS
aldosterone synthase inhibitor FAD286, CYP11B2, extra-adrenal aldosterone, intestinal aldosterone synthesis, intestinal inflammation

1 | INTRODUCTION

The main mineralocorticoid, aldosterone, influences blood pressure by controlling fluid and electrolyte balance; it binds to mineralocorticoid receptors (MR) in the cytosol of the distal tubule and collecting ducts in renal nephrons as well as in colonic epithelial cells and promotes sodium and water reabsorption as well as potassium excretion.[1] By modulating the activity of basolateral Na^+/K^+-ATPase and apical sodium channels in the kidney, aldosterone also regulates electrolyte balance in the colon.[2,3] In the large intestine of the rat, aldosterone upregulates the expression of β and γ subunits of epithelial sodium channels (ENaC) via activation of the MR.[4] Knockout of intestinal MRs in mice decreased the expression of these subunits, leading to a reduction of the animals' blood pressure.[5]

Traditionally, aldosterone has been considered to be synthetised from cholesterol in a complex enzymatic chain exclusively in the *zonula glomerulosa* of the adrenal cortex (Figure 1).[2] However, over the past two decades, it has become apparent that this form of steroidogenesis also occurs in many other cells and tissues, including the brain,[6] heart,[7] blood vessels,[8] kidneys[9] and adipocytes.[10] Recently, we reported the presence of locally produced aldosterone in the large intestine of mice. Both the protein and mRNA of aldosterone synthase (CYP11B2), the terminal enzyme involved in aldosterone production, were identified, suggesting that the intestine should be viewed as an aldosteronegenic tissue.[11,12] The biosynthesis of aldosterone in the intestine seemed to be increased by the same driving factors as those functioning in the adrenal *zona glomerulosa*, that is, sodium deficiency, angiotensin II (Ang II) and the second messenger of adrenocorticotropic hormone (ACTH), cyclic adenosine 3′,5′-monophosphate (cAMP).[12,13] Our working hypothesis is that locally produced aldosterone, functioning in a paracrine manner, would be able to exert an impact on the extent of Na^+ reabsorption and K^+ excretion in the colon. This hypothesis is supported by an experiment where Ang II incubation increased sodium and water transfer in the jejunum of adrenalectomised and nephrectomised rats.[14]

There is a growing body of evidence recognising the importance of locally produced aldosterone in pathophysiological conditions.[7,15–17] Therefore, investigations aiming to assess the therapeutic capacity of aldosterone inhibition have started to emerge. Fadrozole (FAD286), a selective CYP11B2 blocker, is able to decrease aldosterone production efficiently in rats without affecting the level of corticosterone.[18,19] Treatment with FAD286 attenuated the elevated local aldosterone production and signs of inflammation in the kidneys of diabetic rats, providing evidence that the compound may possess renoprotective effects.[17] Similarly, FAD286 decreased the mechanical hypersensitivity of dorsal root ganglia[20] and neovascularisation in oxygen-induced retinopathy, along with upregulating local CYP11B2 activity.[21]

The levels of tight junction proteins are altered,[22,23] and intestinal permeability is increased in inflammatory bowel disease (IBD),[24] and this phenomenon is mimicked in the dextran sodium sulphate (DSS)-induced intestine inflammatory murine model.[25] In addition, aldosterone has been linked to changes in the permeability of barrier tissues; for example, it has been shown to increase vascular permeability in rats' skin[26] and human umbilical vein endothelial cells.[27] In contrast, in the colon, aldosterone has been claimed to decrease the permeability of colonic crypt cells to macromolecules like fluorescein isothiocyanate (FITC)-labelled dextran (10 kDa) under low-sodium conditions.[28]

The pathophysiological relevance of intestinal aldosterone production is still far from clear. This preclinical study aimed to test the hypothesis that FAD286 could be used to attenuate DSS-induced inflammation by inhibiting intestinal aldosterone production. Given the importance of disturbances in intestinal barrier function in IBD, this study also assessed the impact of aldosterone production on intestinal permeability.

2 | MATERIALS AND METHODS

2.1 | Animals and ethical licence

The study was conducted in accordance with the Basic and Clinical Pharmacology and Toxicology policy for experimental and clinical studies.[29] Ethical approval was

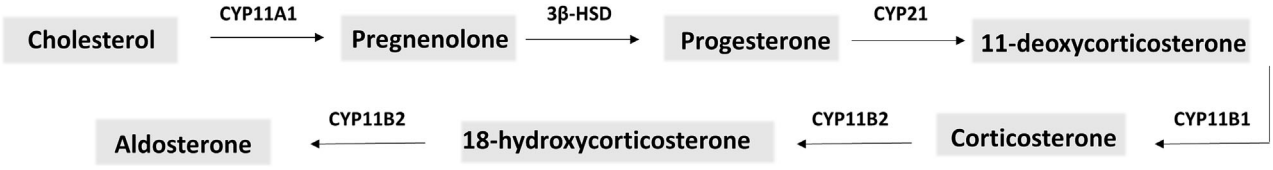

FIGURE 1 Illustration of the metabolic pathway from cholesterol to aldosterone.

obtained from the Regional State Administrative Agency for Southern Finland (ESAVI/9377/2019) in accordance with the Finnish Experimental Animal Act 62/2006. This included measures to reduce animal distress, pain, and suffering. Thirty-six four-week-old male Sprague-Dawley rats (Janvier, Le Genest-Saint Isle, France) were pair-housed in individually ventilated cages and maintained in an artificial 12:12 h light/dark photoperiod, with an average room temperature of 22 ± 2°C and humidity of 55%. The rats had free access to standard rodent chow (Teklad Global 18% Protein Rodent Diet, Harlan Laboratories, Madison, WI, USA) throughout the study.

2.2 | Study protocol

After a six-day-long acclimatisation period, the animals were randomly assigned to four experimental groups: (1) control ($n = 8$); (2) DSS ($n = 10$); (3) DSS + FAD286 ($n = 10$); and (4) FAD286 ($n = 8$). The group sizes were based on pharmacological practice and experience. The control and DSS groups received 0.9% saline injections subcutaneously (s.c.) daily for 12 days, whereas the DSS + FAD286 and FAD286 groups were dosed s.c. with FAD286 (30 mg/kg/d) as a racemate (provided and synthetized by Boehringer Ingelheim Pharma GmbH & Co., Ingelheim, Germany) in 0.9% saline (Figure 2). After 3 days of pre-treatment injections with FAD286 or saline, acute colitis was induced in the DSS and DSS + FAD286 groups by administration of 5% (w/v) DSS 40 kDa (TdB Labs, Uppsala, Sweden) in the rats' drinking water for 7 days (days 3 to 10). Controls were given water ad libitum throughout the study, while the DSS groups had free access to water prior to the induction of colitis. The doses of DSS and FAD286 were chosen based on a pilot study as well as previously published literature.[19,21,30,31] DSS has been shown to interfere with reverse transcriptase quantitative polymerase chain reaction (RT-qPCR) measurements by inhibiting the activity of the reverse transcriptase enzyme, and therefore a two-day wash-out period with water ad libitum was included after DSS administration prior to euthanasia.[32] Rectal bleeding was observed throughout the study and scored on a scale of 0–2, where 0 indicates no bleeding, 1 indicates mild bleeding, and 2 indicates considerable bleeding.

2.3 | Permeability measurement in vivo

On the experimental day 11 rats were given 1 ml of iohexol (Omnipaque 300™, 647 mg iohexol/ml, GE Healthcare, Oslo, Norway) by oral gavage to assess the level of intestinal permeability. The urine was collected in metabolic cages during 24 h, the volumes measured prior to storage at −80°C. The urinary concentration of iohexol was measured with an Enzyme-linked immunosorbent assay (ELISA) kit (BioPAL Inc., Worcester, MA, USA) and the iohexol permeability percentage was calculated by dividing the amount of iohexol in the urine sample by the administered iohexol dose (mg).

2.4 | Tissue collection

Following euthanasia under isoflurane anaesthesia (4%, Vetflurane, Virbac, Carros, France), the colon was immediately removed, its length measured, opened longitudinally and photographed for macroscopical evaluation. The tissue was then gently cleansed with phosphate-buffered saline (PBS) (137 mM NaCl, 10 mM Na_2HPO_4, 2.7 mM KCl, pH = 7.4) to remove any visible blood and intestinal contents before it was snap-frozen in liquid nitrogen and stored at −80°C. Adrenal glands were also collected and weighed.

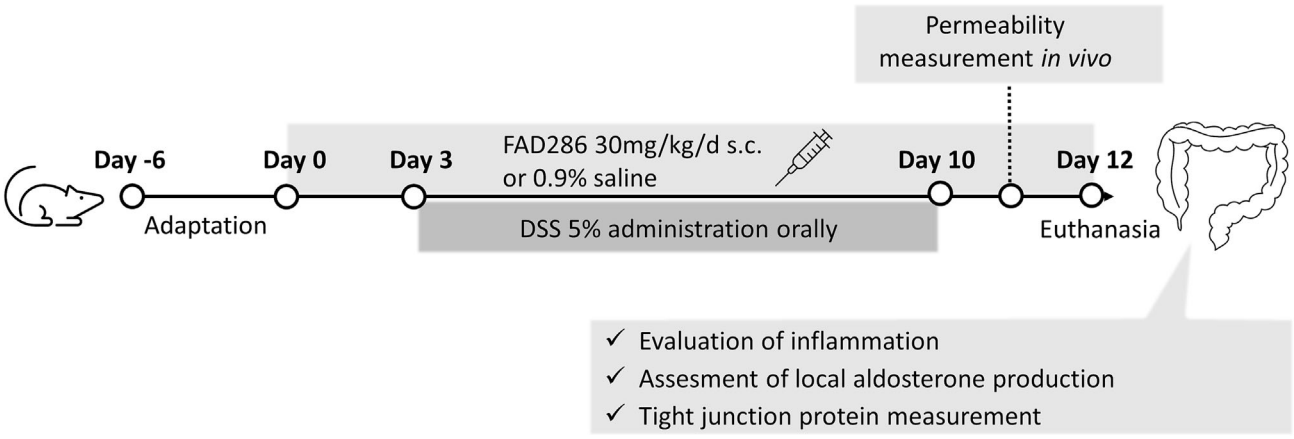

FIGURE 2 The study design and workflow.

2.5 | Macroscopical evaluation of inflammation

Three researchers (RK, HV and LL) evaluated the degree of inflammation from images by assessing the following parameters on a 0–3 scale: the presence of diarrhoea and visible signs of blood to create an inflammatory score, including possible edema and ulcerations.[33,34] To control for bias, the evaluation was performed independently and in a blind manner.

2.6 | Histopathology

An approximately 1-cm-long piece from the distal colon was opened longitudinally, fixed in 4% paraformaldehyde (Scientific, Waltham, MA, USA) solution for 36 h and then stored at +4°C in 70% EtOH until histological processing. The fixed samples were cut into two longitudinal halves; these were embedded in paraffin and cut into 4 μm thick sections. The sections were stained with haematoxylin and eosin (HE) dyes.

Histopathological findings were evaluated by an experienced veterinary pathologist (JL), who examined HE-stained sections using a grading system based on a protocol devised by Wirtz et al.[35] Shortly, the tissue damage and inflammatory cell infiltration were separately scored using integer scores 0–3 summed to a combined score ranging from 0 to 6, where 0 indicates no damage and 6 refers to extensive damage in the bowel wall as well as wide-spread transmural infiltrations. The scoring was slightly modified to account for the FAD286-induced oedema by increasing the tissue damage score by 0.5 points in samples showing mucosal and/or submucosal oedema. In selected samples, the HE stain was augmented with an immunohistochemical assessment of macrophages using the anti-Iba1 (AIF-1) antibody, T-lymphocytes using the anti-CD3 antibody and B-lymphocytes using the CD79a antibody (see below). The pathologist was aware of the study design and which animals belonged to the same group but was blinded by the treatments of the groups.

2.7 | Immunochemical measurements and immunohistochemistry

Samples from the distal colon and adrenal glands were homogenised in ELISA buffer (136 mM NaCl, 8 mM Na_2HPO_4, 2.7 mM KCl, 1.46 mM, KH_2PO_4, 0.001% tween, pH 7.4) with a Precellys homogeniser (Bertin Technologies, Montigny le Bretonneux, France) followed by sonication (17 kHz, 10 s). The Pierce™ BCA protein assay kit (Thermo Fischer Scientific, Waltham, MA, USA) was used in the estimation of the total protein concentration. The homogenised samples were centrifuged and supernatants, diluted to the same protein concentrations, were then assayed for aldosterone and corticosterone ('tissue concentrations') using ELISA kits (#501090 and #501320, Cayman Chemical, Ann Arbor, MI, USA). TNF-α was analysed from the supernatants with an ELISA kit purchased from Elabscience (Houston, TX, USA). The TNF-α concentrations were normalized against tissue total protein. ELISA measurements were done on the same day for each analysis.

For immunohistochemistry, deparaffinised sections were first incubated for 20 min at 99°C in 10 mM citrate buffer (pH 6) for antigen retrieval. The primary rabbit polyclonal antibodies, Iba1 (FUJIFILM Wako Chemicals, Neuss, Germany; dilution 1:500), CD3 (Agilent Dako, Agilent, Santa Clara, CA, USA; dilution 1:400) and monoclonal mouse Ab CD79a (Bio-Rad Finland, Helsinki, Finland; clone HM57; 1:400), were incubated at RT for 60 min. Vectastain ABC-HRP kit (Vector Laboratories, Burlingham, CA, USA) with biotinylated anti-rabbit or anti-mouse antibody and DAP substrate were used for detection according to the manufacturer's instructions.

2.8 | Western blot

A Western blot was performed using distal colon pieces according to the protocol described in detail previously.[12] The primary antibodies used to detect the CYP11B2 and tight junction proteins were as follows: anti-CYP11B2 (ab167413, 1:100, Abcam, Cambridge, UK), claudin-1 (A-9, 1:100; Santa Cruz Biotechnology, Dallas, TX, USA), claudin-2 (3F1, 1:200; Santa Cruz Biotechnology), claudin-4 (A-12, 1:100; Santa Cruz Biotechnology) and occludin (40-4700, 1:100; Invitrogen, Waltham, MA, USA). The secondary antibodies, IRDye680LT and IRDye800CW, were purchased from Li-COR (Lincoln, NE, USA). The band intensities were measured using the Odyssey CLx InfraRed system (Li-COR). The intensities of all target protein bands were normalized to the intensity of β-actin (3700S, 1:3000; Cell Signalling Technology, Danvers, MA, USA), except for CYP11B2, which was normalized to glyceraldehyde-3-phosphate dehydrogenase (GAPDH) (1:1000, cell signalling). The colon control group was standardised as unity, with protein expression in the other groups being compared to that value.

TABLE 1 Primer sequences used in the measurements.

Gene	Forward primer (5′-3′)	Reverse primer (5′-3′)	Product size (pb)	Ref.
GAPDH	GCTGCCTTCTCTTGTGACAA	ATCTCGCTCCTGGAAGATGG	183	36
β-actin	AGATCAAGATCATTGCTCCTCCT	AAAACGCAGCTCAGTAACAGT	177	36
LDHA	CATCGTGCACTAAGCGGTCC	GCAAGCTCATCAGCCAAGTC	186	37
CYP11B2	AGAAGCTTGACTCGCTGGAC	TTAGTGCTGCCACAATGCCA	157	
TNF-α	AAATGGGCTCCCTCTCATCAGTTC	TCTGCTTGGTGGTTTGCTACGAC	111	38
Il-1β	CACCTTCTTTTCCTTCATCTTTG	GTCGTTGCTTGTCTCTCCTTGTA	241	39
Il-6	TCCTACCCCAACTTCCAATGCTC	TTGGATGGTCTTGGTCCTTAGCC	79	38
COX-2	CATGATCTACCCTCCCCACG	CAGACCAAAGACTTCCTGCCC	67	37

Abbreviations: COX-2, cyclooxygenase 2; CYP11B2, aldosterone synthase; GAPDH, glyceraldehyde-3-phosphate dehydrogenase; Il-1β, interleukin 1 beta; Il-6, interleukin 6; LDHA, lactate dehydrogenase; TNF-α, tumour necrosis factor alpha.

2.9 | RT-qPCR

The gene expression levels of CYP11B2, TNF-α, Il-1β, Il-6 and COX-2 (PTGS2) were evaluated using RT-qPCR. First, the RNA was extracted from approximately 30 mg of colon and pooled adrenal gland tissue using the NucleoSpin RNA kit (Macherey Nagel, Duren, Germany), and the quality and concentration were analysed with a NanoDrop spectrophotometer (Thermo Fisher). RT-qPCR measurements were accomplished using cDNA generated from 1 μg of extracted RNA with the iScript cDNA Synthesis Kit (Bio-Rad). The primer pair for CYP11B2 (Table 1) was created in Primer-BLAST (NCBI, Bethesda, MD, USA) and custom-made by Sigma-Aldrich (St. Louis, MO, USA). For the other primers, a reference is provided. All primers were tested against any non-specific amplification using a dilution series of a pooled sample of colon cDNA.

RT-qPCR reactions were carried out on the LightCycler 96 (Roche Diagnostics GmbH, Penzberg, Germany) and amplified with the LightCycler 480 SYBR Green I Master (Roche Diagnostics GmbH). The running parameters were as follows: pre-denaturation (10 min at 95°C), followed by 40 cycles of denaturation (15 sec at 95°C), annealing (30 sec at 60°C) and extension (30 sec at 72°C). To confirm the specificity of the primers, melting curves were evaluated after each run. Results were assessed as normalized relative quantities (NRQ) according to the Vandesompele procedure[36] and normalized using three housekeeping genes: GAPDH, β-actin and lactate dehydrogenase (LDHA).

2.10 | Statistics

Significance levels were set at $p < 0.05$ using a one-way ANOVA followed by Tukey's post-hoc test. The body weight changes between the groups were compared using a two-way ANOVA. The correlation between the percentage incidence of gastrointestinal bleeding and the change in iohexol permeability, evaluated as a percentage, was assessed using Spearman's correlation. Statistical assessments were conducted, with the graphical representations created by GraphPad Prism 8 by Dotmatics. Data are presented as mean ± standard error of the mean (SEM), except for the RT-qPCR results, which are shown as the geometric mean. Grubb's test was used to detect and exclude outliers.

3 | RESULTS

3.1 | Body weight and inflammation

In order to investigate the severity of intestinal inflammation, the weight gain, the length of the colon and macroscopical signs of inflammation, as well as the presence of gastrointestinal bleeding, were analysed. The weight and well-being of the animals were monitored daily. No statistical differences were present in the body weights of the four groups at the beginning of the experiment: control (219.4 ± 6.2 g), DSS (222.6 ± 7.6 g), DSS + FAD286 (227.6 ± 7.1 g) and FAD286 (220.9 ± 3.9 g). DSS consumption reduced the body weight gain compared with the control group from the first day after DSS administration, whereas FAD286 alone did not alter the gain in body weight (Figure 3A). At the end of the study, the weight gain of the rats receiving DSS + FAD286 was less than the weight gain of the animals administered DSS. No significant differences were detected between the groups in their daily fluid consumption (Figure S1).

The length of the colon was shorter in the DSS group when compared to control rats ($p < 0.05$) (12.3 ± 0.4 cm vs. 14.1 ± 0.5). The effect was not abolished by treatment with FAD286 (11.8 ± 0.3 cm) (Figure 3B,C). The length of the colon was unaffected by FAD286 alone (14.5

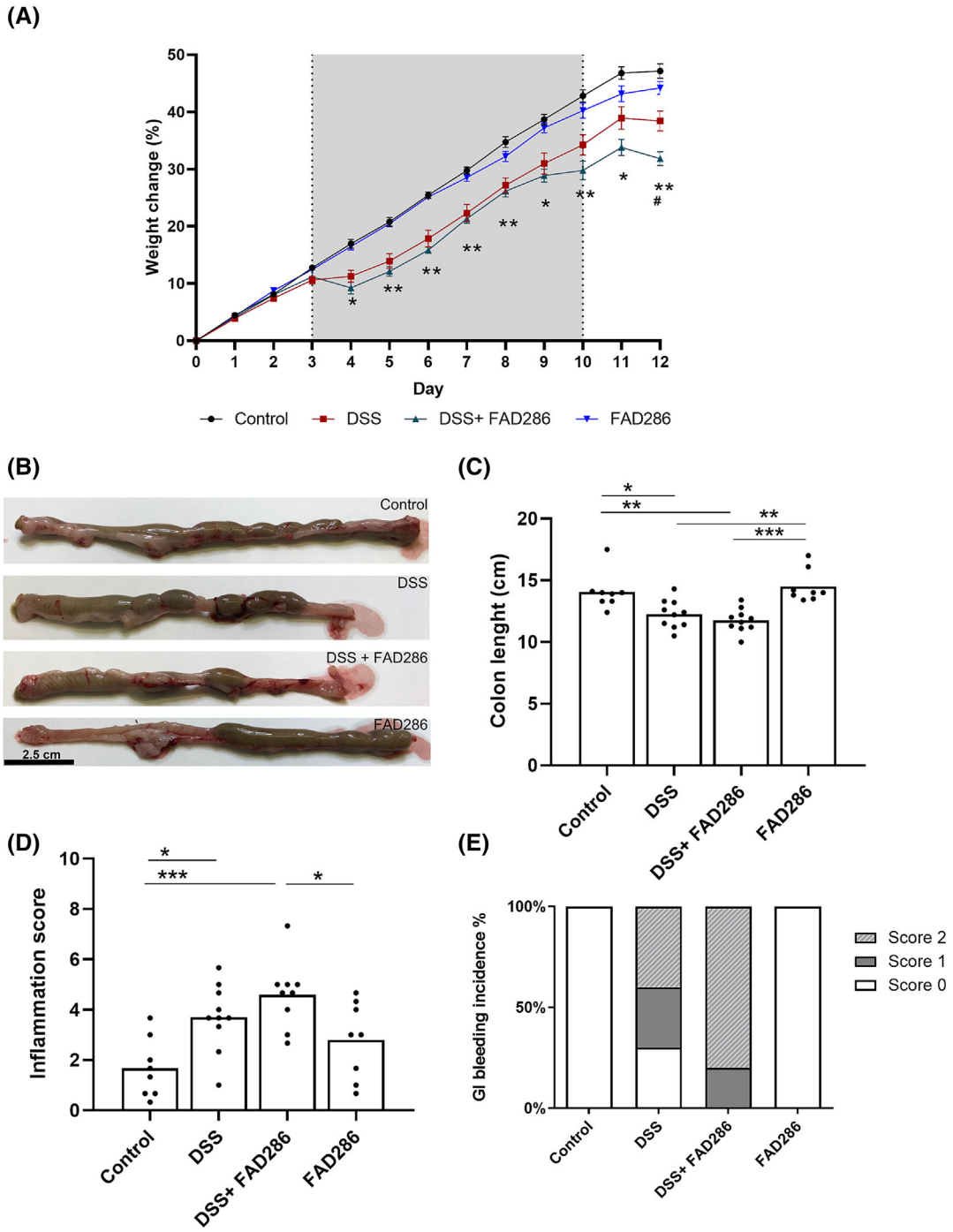

FIGURE 3 (A) Body weight percentage differences throughout the experiment. The grey zone demonstrates the administration of dextran sulphate sodium (DSS). Groups are compared with a repeated two-way ANOVA followed by Tukey's post-hoc test. * denotes $p < 0.05$ DSS compared to healthy control; ** denotes $p < 0.01$ DSS compared to healthy control; # denotes $p < 0.05$ DSS compared to DSS + fadrozole (FAD286) group; $n = 8$–10/group. (B) Representative macroscopic images of colon specimens from representatives of the four groups. (C) The length of colon (cm). (D) Blinded macroscopic evaluation by three researchers (total score 0–9). (E) Observed rectal bleeding (GI) in vivo (%). 0 = no bleeding; 1 = mild bleeding; 2 = considerable bleeding. C and D Arithmetic mean, $n = 8$–10/group, *$p < 0.05$; **$p < 0.05$; *** $p < 0.001$.

± 0.4 cm). The macroscopical evaluation revealed that DSS increased the inflammation score (consistency of faeces, presence of blood and oedema) compared to control animals (Figure 3D and Figure S2). On the other hand, when the animals received FAD286 while they were consuming DSS, this combination seemed to further exacerbate the signs of inflammation. The most intense bleeding in the colon was evident in the DSS + FAD286

group, where 80% of the animals experienced considerable bleeding, with the remaining 20% showing evidence of mild bleeding (Figure 3E). In the DSS group, 40% had considerable rectal bleeding; in 30%, bleeding was assessed as mild. Finally, there were no signs of any bleeding in the colons of control or FAD286 treated rats.

3.2 | Histological analysis

No histological lesions were observed in the control rats, whereas FAD286 administration alone (0.6 ± 0.2) caused mild oedema in the lamina propria and submucosa (Figures 4 and 5A,B). The DSS-treated animals showed evidence of mild tissue damage; in general, the inflammation was limited to the mucosa (score = 2.3 ± 0.2) (Figure 5C,D). The surface epithelium exhibited minimal degenerative changes, minimal to mild hyperplasia and regeneration in the crypt epithelia, and signs of mild lymphoplasmacytic infiltration with granulocytes and/or Iba-1-positive macrophages were present in the lamina propria. Finally, three out of 10 animals in the DSS group showed focal chronic (healing) mucosal ulcers or crypt necrosis and dysplastic regenerative crypt segments. In the DSS + FAD286 group, the histology score (4.9 ± 0.2) was significantly higher than in the DSS animals; in fact, the DSS + FAD286-treated rats generally displayed moderate to severe signs of tissue damage and inflammatory lesions extending to the submucosa and sometimes to the muscularis externa (Figure 5E,F). In this group, the majority (7/10 animals) displayed evidence of chronic mucosal ulcers as well as a mixed inflammatory infiltrate or neutrophilic inflammation and oedema in the submucosa. One rat was assessed to have focal mucosal necrosis with submucosal purulent inflammation, and one animal exhibited signs of transmural necrosis. However, despite moderate-to-marked neutrophil infiltration and minor haemorrhages in the lamina propria, the surface epithelium exhibited minimal-to-no degenerative changes, and the epithelia exhibited regenerative hyperplasia outside of the necrotic and ulcerated areas.

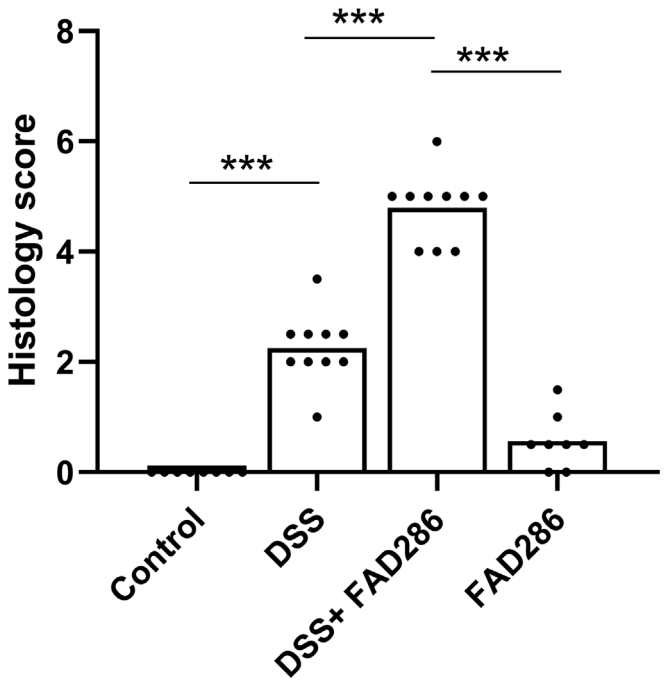

FIGURE 4 Histology scores of the distal colon from control, dextran sodium sulphate (DSS)-treated, DSS + fadrozole (FAD286) and FAD286 rats. Arithmetic mean, n = 8–10/group.

3.3 | Inflammatory markers

Unexpectedly, DSS as well as DSS + FAD286 animals exhibited significantly lower distal colonic TNF-α levels as compared to the control rats on the second day after the end of DSS administration (Table 2). FAD286 combined with DSS further decreased the TNF-α concentration in comparison with the DSS animals. The gene expression levels of three proinflammatory markers, that is, TNF-a, Il-1β, Il-6 and the prostanoid synthesizing enzyme COX-2, measured from the midsection of the colon were not altered statistically significantly.

3.4 | Aldosterone and corticosterone in colon tissue

Elisa assays from homogenised colon tissue supernatants were performed to assess the effect of inflammation on intestinal aldosterone and corticosterone concentrations. The lowest aldosterone concentration (360.9 ± 76.8 pg/ml) was detected in the control group, while rats receiving FAD286 alone had two-fold higher levels (765.4 ± 89.9 pg/ml) (Figure 6A) ($p < 0.05$). In the DSS and the DSS + FAD286 animals, the aldosterone concentrations were elevated as compared to the control group, although in neither group did the difference reach statistical significance. In the adrenal glands, DSS administration elevated the aldosterone concentration by one fourth, while FAD286 treatment decreased it by half vs. control (Figure 6B).

Corticosterone concentrations were measured from the colon and the adrenal glands in order to verify the selectivity of FAD286 treatment between CYP11B1 and CYP11B2 (Figure 6C, D). The measurement revealed that the corticosterone levels in both tissue homogenates were unaffected by FAD286 treatment. In the DSS + FAD286 group, the corticosterone concentration in the colon tended to be higher than in the control group ($p = 0.059$).

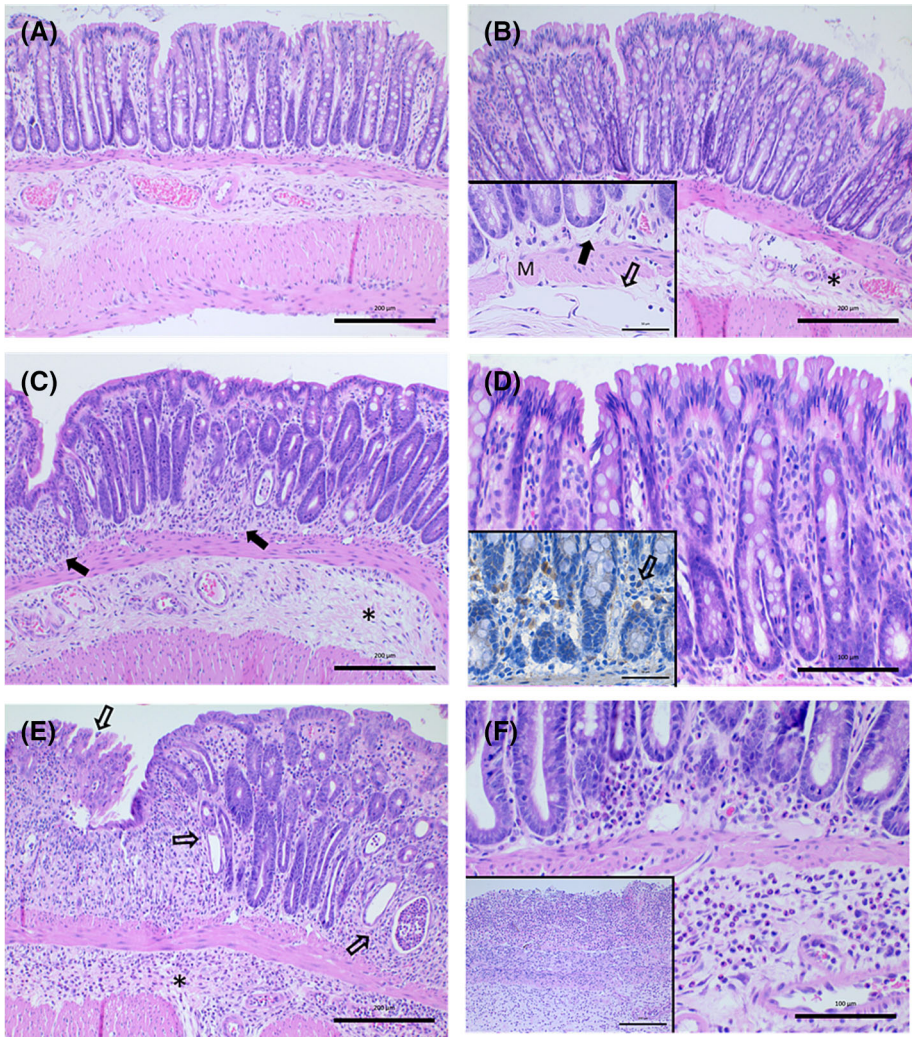

FIGURE 5 Representative microphotographs of haematoxylin and eosin (HE)-stained sections of control-, fadrozole (FAD286)-, dextran sodium sulphate (DSS)- and DSS + FAD286-administered rats. (A) Control rat colon. Bar 200 μm. (B) FAD286-induced edema in the submucosa (asterisk) and in the basal mucosa. Bar 200 μm. Inset: close-up of the edema in the lamina propria below the crypt bases (arrow) and loose edematous submucosa with a dilated lymphatic vessel (open arrow), separated by muscularis mucosae (M). Bar 50 μm. (C) DSS-treated rat. Two small chronic, healing mucosal ulcers (arrows) showing neutrophil and macrophage infiltration. The surface epithelium and the crypts exhibit regenerative hyperplasia (basophilia, cell crowding and increased number of mitoses). Lamina propria displays a modest mixed inflammatory infiltrate, but no infiltrate is present in the submucosa (asterisk). Bar 200 μm. (D) DSS-treated rat showing typical minimal changes in the mucosa. Mildly increased number of lymphocytes in the lamina propria, minimal crypt and surface epithelial hyperplasia. Bar 100 μm. Inset: CD79a-reactive B-lymphocytes (open arrow) in the lamina propria. Bar 50 μm. (E) DSS + FAD286-treated rat. Chronic, healing ulcerated area showing neutrophil and macrophage infiltration and crypt remnants. The surface epithelium and the crypts exhibit degeneration, dysplasia and a crypt abscess in the immediate vicinity of the ulcer (open arrows). Lamina propria displays a purulent inflammatory infiltrate that spreads to the submucosa (asterisk). Bar 200 μm. (F) DSS + FAD286-treated rat. Purulent infiltrate in the lamina propria and submucosa in a moderately affected colon segment; no ulceration. Bar 100 μm. Inset: necrotic colon wall with mixed inflammatory infiltrate. Bar 200 μm.

3.5 | CYP11B2

Western blot analysis of the protein levels of CYP11B2 from the colon and the pooled adrenal gland homogenates detected a non-significant ($p = 0.08$) decrease in CYP11B2 expression in the DSS group as compared with control rats (Figure 7B). In the pooled adrenal gland samples, the alterations between groups were less than 20%. The most intriguing aspect of this data is that the size of CYP11B2 in the colon seemed to be approximately 5 kDa smaller than its counterpart in the adrenal gland (Figure 7A and Figure S3).

TABLE 2 (A) Tumour necrosis factor alpha (TNF-α) protein level in distal colon supernatant (pg/mg total protein) (mean ± SEM, $n = 8–10$ in each group). (B) TNF-α, interleukin 1 beta (Il1-b), interleukin 6 (Il-6) and cyclooxygenase 2 (COX-2) gene expression as related to the control group in the midsection of the colon 2 days after the end of the DSS treatment. The data is expressed as a geometric mean, and the confidence interval is provided, $n = 7–10$ in each group.

		Target	Control (C)	DSS (D)	DSS + FAD286 (DF)	FAD286 (F)	Statistics $p < 0.05$
A	Protein (pg/mg)	TNF-a	12.2 ± 1.2	8.7 ± 0.7	4.0 ± 0.8	11.4 ± 0.9	C vs. D, C vs. DF, D vs. DF, DF vs. F
B	Gene	TNF-α	1 (0.3–1.8)	0.71 (0.4–1.1)	0.55 (0.3–1.0)	0.82 (0.3–2.2)	-
		Il-1β	1 (0.7–1.2)	0.69 (0.2–2.2)	0.51 (0.1–1.7)	0.71 (0.4–1.2)	-
		Il-6	1 (0.8–1.4)	0.67 (0.4–1.4)	0.95 (0.2–1.9)	1.05 (0.7–2.3)	-
		COX-2	1 (0.7–1.8)	0.97 (0.4–2.1)	0.85 (0.4–2.3)	0.92 (0.3–1.5)	-

Abbreviations: DSS, dextran sodium sulphate; FAD286, fadrozole; SEM, standard error of the mean.

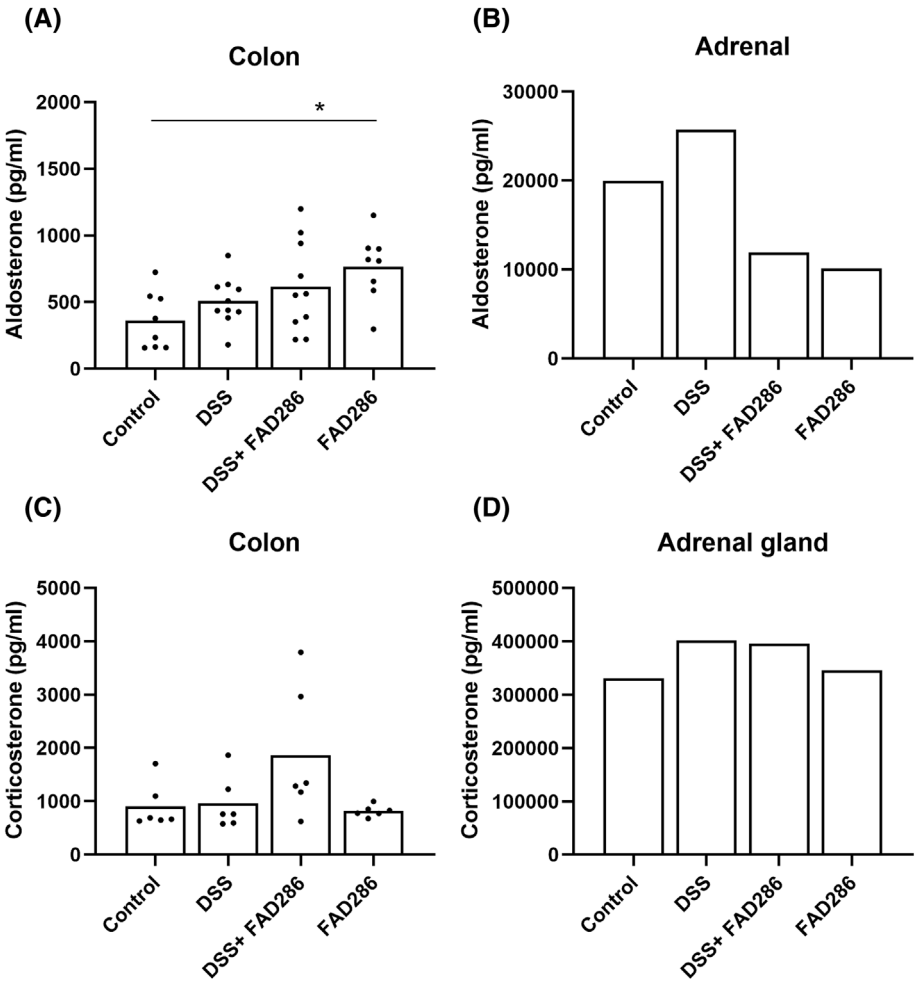

FIGURE 6 Levels of aldosterone from colon tissue supernatants diluted to the same protein concentration were measured using ELISA (A) and adrenal gland samples (B). Corticosterone levels in the supernatant of colon homogenate (C) and in the adrenal glands (D) were measured using ELISA. $n = 8–10$ in each colon aldosterone group and $n = 6$ in each colon corticosterone group (arithmetic mean), pooled sample of adrenal glands from three animals in each group, $^*p < 0.05$.

3.6 | CYP11B2 gene expression

DSS appeared to lower the gene expression of CYP11B2 in comparison to control (Figure 8), and this decrease was even more extensive in the animals treated with combined DSS and FAD286 ($p < 0.01$). The adrenal gland controls contained a much higher concentration of aldosterone than the colon, as much as 6000 times greater when measured in terms of the tissue protein level. Interestingly, in the adrenal glands, both groups receiving FAD286 treatment showed considerably lower levels of CYP11B2 mRNA, while in the DSS animals, the expression was increased by one-third over the control level.

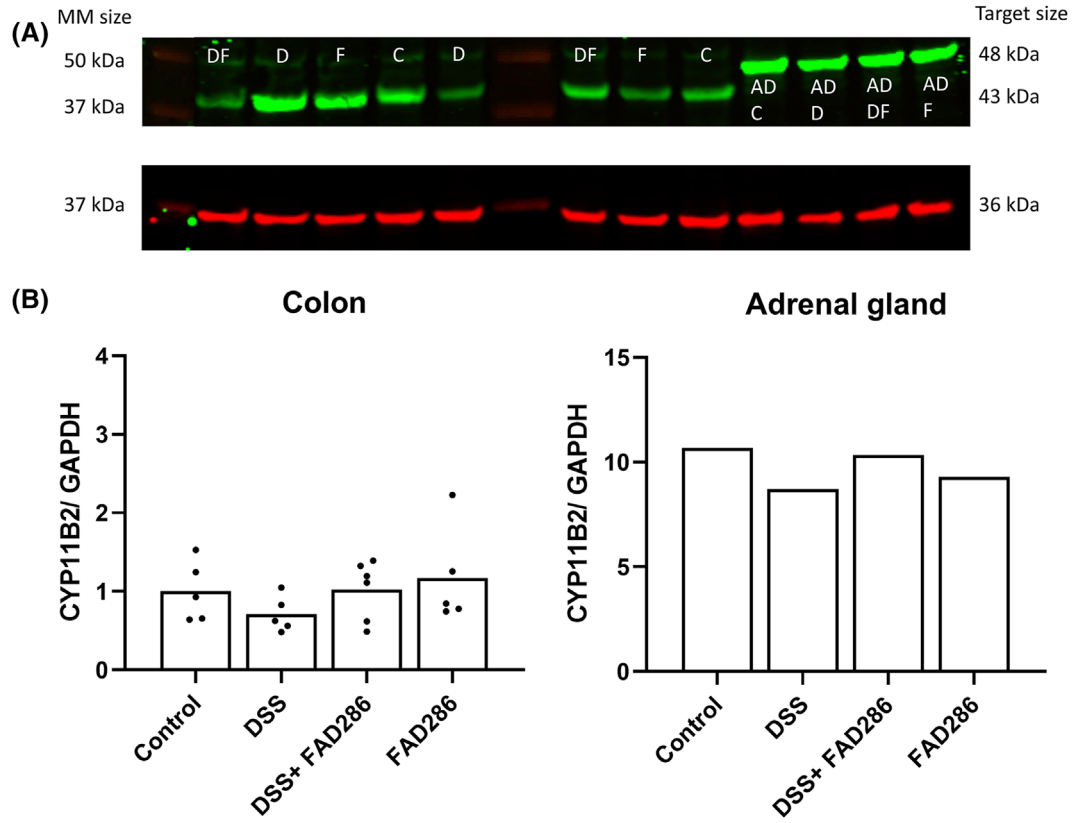

FIGURE 7 (A) Representative images of aldosterone synthase (CYP11B2) (green) and glyceraldehyde-3-phosphate dehydrogenase (GAPDH) (red) protein bands on Western blot membrane. AD = adrenal gland, D = DSS, DF = DSS + FAD286, F = FAD286, MM = molecular weight marker. (B) CYP11B2 levels in control, dextran sodium sulphate (DSS), DSS + fadrozole (FAD286) and FAD286 groups were analysed from distal to the midsection of the colon and pooled adrenal glands from three animals. n = 5–6/colon group (arithmetic mean).

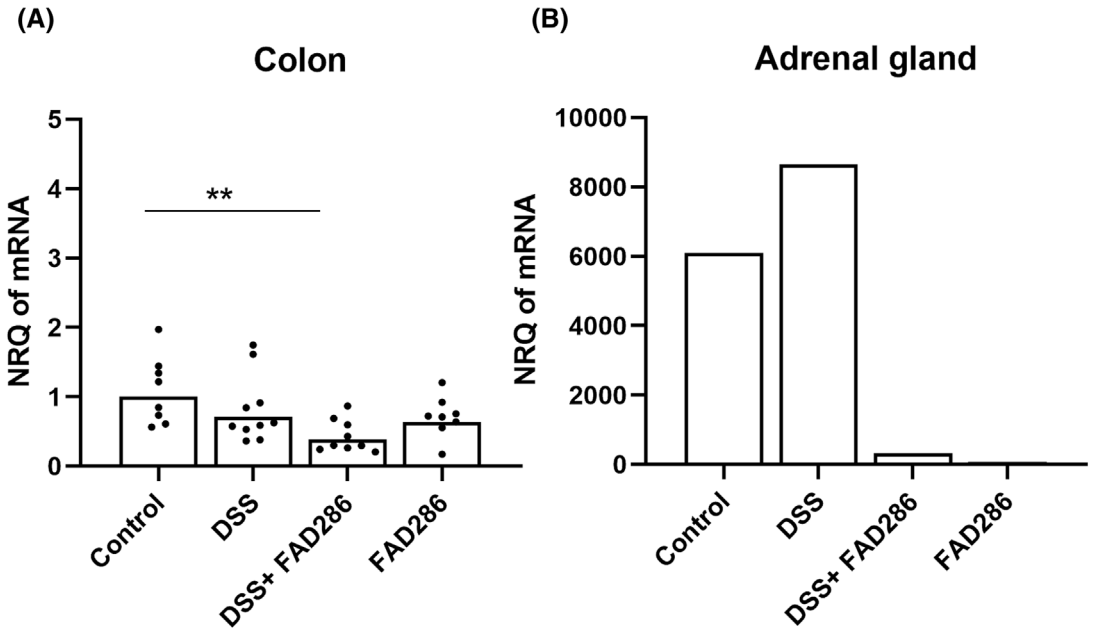

FIGURE 8 Gene expression of aldosterone synthase (CYP11B2) in the colon (n = 8–10/group) (A) and in the pooled sample of adrenal glands from three animals (B). The data is shown as a geometric mean, $^{**}p < 00.1$. NRQ, normalized relative quantity. The colon is normalized to 1.

3.7 | Intestinal permeability

We assessed if aldosterone inhibition altered intestinal permeability by performing an iohexol assay. Permeability to iohexol, measured as a percentage of the administered dose relative to the amount excreted in urine in 24 h, was significantly higher in the DSS + FAD286 group (12.4 ± 2.2%) in comparison to the other groups (Figure 9A). DSS (4.8 ± 0.4%) and FAD286 treatments alone (4.2 ± 0.3%) increased iohexol permeability as compared to the control group (2.7 ± 0.2%), but this was not statistically significant. The incidence of gastrointestinal bleeding from the rectum correlated positively with iohexol permeability (Spearman's rho = 0.749, $p < 0.001$) (Figure 9B).

3.8 | Tight junction proteins

There were no statistical differences between the groups in the levels of three barrier-strengthening tight junction proteins, that is, claudin-1, claudin-4 and occludin (Table 3), although a decreasing trend was observed in the occludin level in the DSS-treated group. No marked differences between the groups were detected in the pore-forming protein claudin-2. The bands of each protein are shown in the supplementary data (Figure S4).

4 | DISCUSSION

This study aimed to investigate the role of intestinal aldosterone production in the development of intestinal inflammation. We used the DSS-induced colitis rat model and CYP11B2 inhibitor, FAD286, to investigate whether inhibition of aldosterone production would influence intestinal inflammation in the colon. As a result, we showed that FAD286 treatment aggravated the extent of intestinal inflammation in an inflamed intestine. However, FAD286 did not lower colonic aldosterone levels. FAD286 treatment had no clear impact on intestinal inflammation in a healthy intestine.

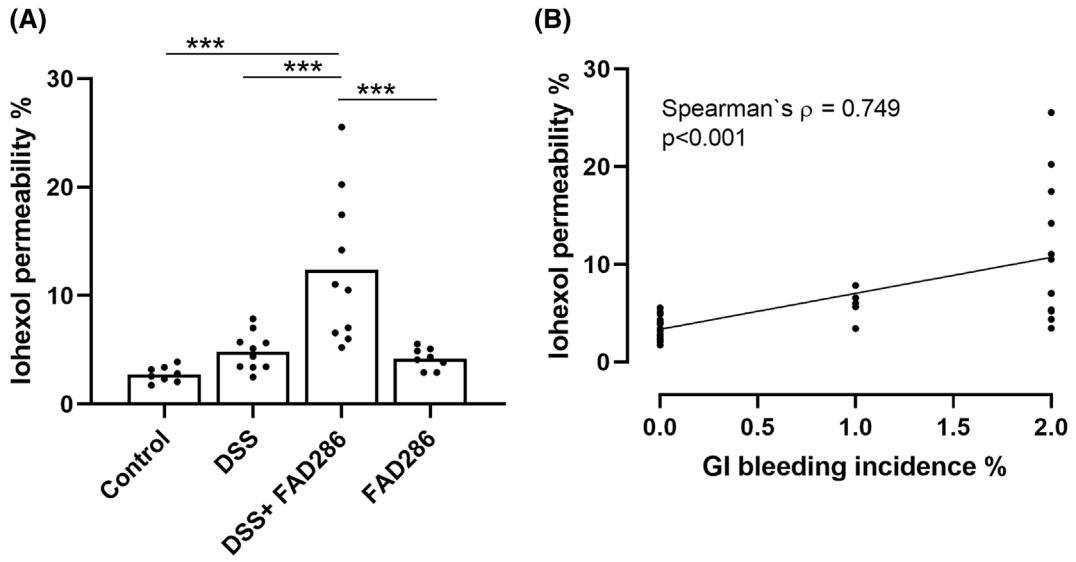

FIGURE 9 (A) Intestinal permeability percentage in urine of an administered dose of iohexol. $n = 8$–10/group (arithmetic mean), ***$p < 0.001$. (B) Spearman's correlations between the incidence of gastrointestinal (GI) bleeding and iohexol permeability (Spearman's rho = 0.749, $p < 0.001$).

TABLE 3 The levels of tight junction proteins claudin-1, claudin-4 and occludin, as well as the pore-forming protein claudin-2, were analysed from the distal colon and related to the control in the different treatment groups as measured with Western blot. Mean ± SEM, $n = 6$–7 in each group.

	Control	DSS	DSS + FAD286	FAD286
Claudin-1	1 ± 0.11	0.89 ± 0.07	0.90 ± 0.16	1.26 ± 0.15
Claudin-2	1 ± 0.14	1.17 ± 0.16	1.05 ± 0.18	1.03 ± 0.12
Claudin-4	1 ± 0.13	1.11 ± 0.17	1.18 ± 0.18	1.10 ± 0.09
Occludin	1 ± 0.15	0.73 ± 0.09	0.94 ± 0.16	1.00 ± 0.15

Abbreviations: DSS, dextran sodium sulphate; FAD286, fadrozole

Previous research has associated increased local aldosterone synthesis with several pathophysiological conditions,[7,15–17,40] including inflammation; it has been shown that these symptoms could be attenuated by administering FAD286.[17,20,21] Based on these findings and on our previous reports indicating that the intestine is aldosteronegenic,[11–13] we hypothesized that the concentration of locally synthetized aldosterone would increase during intestinal inflammation. In fact, this phenomenon was shown to occur in the intestine with respect to corticosterone, the precursor of aldosterone.[41,42] In a previous study, inhibition of RAS at the level of angiotensin converting enzyme (ACE) or Ang II receptor type 1 (ATR1) alleviated DSS-induced colitis.[43] Therefore, in the present study, we speculated that FAD286 would have beneficial effects on intestinal inflammation by preventing the elevated production of aldosterone. As intestinal permeability is increased in the rodent DSS model[25] as well as in IBD,[24] we also evaluated whether inhibition of aldosterone in the DSS model could influence the permeability of larger molecules.

As expected, in the present study, we observed that the inflammation induced by DSS manifested as decreased body weight gain, a shortened colon length, increased gastrointestinal rectal bleeding, as well as exacerbated macroscopical and histological scores. Contrary to our hypothesis that FAD286 would exert beneficial effects on intestinal inflammation, the compound triggered adverse effects in the DSS animals. The DSS + FAD286 group had a lower body weight gain, increased intestinal bleeding and an increase in permeability to iohexol when compared to the DSS group. FAD286 also aggravated both macroscopic and histological signs of inflammation and tissue damage. The increased bleeding in the DSS + FAD286 treated animals could be explained by the reported prothrombotic effects of aldosterone,[44] which were abolished in the present study by CYP11B2 inhibition seen in adrenal glands (manifested by a clear decrease in aldosterone formation, a slightly lower CYP11B2 protein concentration and the virtual disappearance of mRNA expression).

In the intestine, it is thought that aldosterone exerts its effects via MR.[5] The harmful effects of systemic aldosterone inhibition encountered in our study resemble those described by Johnson et al.,[45] who reported that spironolactone, an MR antagonist that inhibits the effects of aldosterone, increased mortality in two rodent models of intestinal inflammation in a dose-dependent manner. Furthermore, in clinical studies, spironolactone use has been shown to elevate the risk of upper gastrointestinal bleeding and ulcers.[46]

As expected, FAD286 administration significantly decreased the aldosterone concentration in the adrenal glands as compared to control animals. The selectivity of FAD286 to CYP11B2 was indicated by the absence of significant differences in adrenal and colon levels of corticosterone, which are regulated by the isoenzyme CYP11B1. Interestingly, FAD286 did not inhibit intestinal aldosterone synthesis. On the contrary, the highest colonic levels of aldosterone were detected in those animals administered with FAD286. This might be evidence of a compensatory increase in intestinal aldosterone synthesis while systemic aldosterone availability is decreased. The failure of FAD286 to inhibit intestinal aldosterone might be explained by structural differences between colonic and adrenal CYP11B2, seen as a 5 kDa size difference in the molecular weights between those tissues and by differences in the amounts and properties of the enzyme.[12,47] Alternative splicing and polymorphism of CYP11B2 have been previously reported in the literature.[48–50] Therefore, the observed size difference might be due to either gut-specific alternative splicing or post-translational modifications, which could affect the inhibitory properties of FAD286 against the intestinal form of CYP11B2.

We showed, as expected, that colonic permeability was increased in rats with inflammation in that tissue; however, drug treatment with FAD286 increased the permeability even more, which is in line with the results of the macroscopic and histological evaluation of colon inflammation. This kind of increased permeability and an observed decrease in adrenal aldosterone production are in line with an earlier report of alterations in colonic crypt permeability to macromolecules.[28] However, no changes in the current study were seen in the levels of tight junction proteins. This unanticipated result warrants further study. In general, our histological evaluation revealed only modest lesions in contrast to those typically reported in mice,[51,52] as well as marked regenerative hyperplasia in the epithelium outside of the necrotic areas, pointing to a rapid renewal of intestinal epithelium that appears to occur after DSS withdrawal.[53,54]

The CYP11B2 protein levels in the adrenals and colon were unaffected by FAD286 alone vs. the control, while almost a total depression to the zero level was evident in the gene expression of CYP11B2 in the adrenal glands of the rats receiving either only FAD286 or DSS + FAD286. In the colon, only the DSS + FAD286 animals showed a significant inhibition of CYP11B2 expression, although the mean value of the animals treated with FAD286 alone was also lower than in the control group. Thus, as a novel finding, our results show that inhibition of CYP11B2 by FAD286 in adrenal glands extends to the level of regulation of gene expression.

The protein level of TNF-α in the colon decreased in both DSS and DSS + FAD286 groups. This was unexpected, as the histological and macroscopic analyses demonstrated obvious signs of inflammation and tissue

damage. It is possible that a healing process has been initiated during the two-day washout period between the end of DSS administration and euthanasia. However, TNF-α has also been shown to have anti-inflammatory properties, such as stimulation of local glucocorticoid synthesis in situations of intestinal inflammation.[55] Indeed, a TNF-α deficiency has been reported to worsen a colonic injury and decrease the survival rate in a DSS murine model.[56]

DSS disturbs the barrier function of epithelial cells,[57] as was also found in the histological assessment conducted here. Systemic administration of FAD286 alone also evoked mild oedema in the lamina propria and submucosa, an effect that was markedly exacerbated in the DSS group. However, the possibility that the harmful effects of FAD286 in the intestine are generated from the luminal side is unlikely, as the majority of FAD286 is excreted in the urine and not in the bile,[58] and the drug was administered via the subcutaneous route.

In conclusion, intestinal aldosterone does not seem to play a crucial role in the manifold symptoms associated with DSS-induced intestinal inflammation; these could not be prevented by treatment with a selective CYP11B2 inhibitor, FAD286. On the contrary, this drug worsened some of the measured variables. Intestinal CYP11B2 displayed a smaller molecular size compared to its adrenal counterpart and did not inhibit intestinal aldosterone production, which might suggest a different functionality of CYP11B2 between tissues.

ACKNOWLEDGEMENTS

This study was funded by Finska Läkaresällskapet (HL, HV), Mary and Georg C. Ehrnrooth's Foundation (HL), Maud Kuistila Memory Foundation (HL), Paulo Foundation (HL) and Finnish Cultural Foundation (Kymenlaakso regional fund, Olavi and Alli Pietikäinen fund) (LL). We are grateful to Boehringer Ingelheim Pharma GmbH & Co. for providing us with FAD286 and to Dr. Ewen MacDonald for checking the language and style. The personnel of the Finnish Centre for Laboratory Pathology (FCLAP), HiLIFE, are thanked for the histological sample processing and staining.

CONFLICT OF INTEREST STATEMENT

The authors declare no conflict of interest.

ORCID

Hanna Launonen https://orcid.org/0000-0002-5507-8492
Hanne Salmenkari https://orcid.org/0000-0002-3418-152X

REFERENCES

1. Booth RE, Johnson JP, Stockand JD. Aldosterone. *Adv Physiol Educ*. 2002;26(1):8-20. doi:10.1152/advan.00051.2001
2. Connell JMC, Davies E. The new biology of aldosterone. *J Endocrinol*. 2005;186(1):1-20. doi:10.1677/joe.1.06017
3. Harvey BJ, Alzamora R, Stubbs AK, Irnaten M, McEneaney V, Thomas W. Rapid responses to aldosterone in the kidney and colon. *J Steroid Biochem Mol Biol*. 2008;108(3–5):310-317. doi:10.1016/j.jsbmb.2007.09.005
4. Bertog M, Cuffe JE, Pradervand S, et al. Aldosterone responsiveness of the epithelial sodium channel (ENaC) in colon is increased in a mouse model for Liddle's syndrome. *J Physiol*. 2008;586(2):459-475. doi:10.1113/jphysiol.2007.140459
5. Nakamura T, Kurihara I, Kobayashi S, et al. Intestinal mineralocorticoid receptor contributes to epithelial Sodium Channel-mediated intestinal sodium absorption and blood pressure regulation. *J am Heart Assoc*. 2018;7(13). doi:10.1161/JAHA.117.008259
6. Gomez-Sanchez EP, Ahmad N, Romero DG, Gomez-Sanchez CE. Is aldosterone synthesized within the rat brain? *Am J Physiol Metab*. 2005;288(2):E342-E346. doi:10.1152/ajpendo.00355.2004
7. Bose HS, Whittal RM, Marshall B, et al. A novel mitochondrial complex of aldosterone synthase, steroidogenic acute regulatory protein, and Tom22 synthesizes aldosterone in the rat heart. *J Pharmacol Exp Ther*. 2021;377(1):108-120. doi:10.1124/jpet.120.000365
8. Takeda Y, Miyamori I, Yoneda T, et al. Production of aldosterone in isolated rat blood vessels. *Hypertension*. 1995;25(2):170-173. doi:10.1161/01.HYP.25.2.170
9. Xue C, Siragy HM. Local renal aldosterone system and its regulation by salt, diabetes, and angiotensin II type 1 receptor. *Hypertension*. 2005;46(3):584-590. doi:10.1161/01.HYP.0000175814.18550.c0
10. Briones AM, Nguyen Dinh Cat A, Callera GE, et al. Adipocytes produce aldosterone through calcineurin-dependent signaling pathways. *Hypertension*. 2012;59(5):1069-1078. doi:10.1161/HYPERTENSIONAHA.111.190223
11. Varmavuori L, Launonen H, Korpela R, Vapaatalo H. Detection of immunoreactive aldosterone in murine gastrointestinal tract. *J Physiol Pharmacol*. 2020;71(4):597-601. doi:10.26402/jpp.2020.4.15
12. Launonen H, Pang Z, Linden J, Siltari A, Korpela R, Vapaatalo H. Evidence for local aldosterone synthesis in the large intestine of the mouse. *J Physiol Pharmacol*. 2021;72(5):807-815. doi:10.26402/jpp.2021.5.15
13. Pang Z, Launonen H, Korpela R, Vapaatalo H. Local aldosterone synthesis in the large intestine of mouse: an ex vivo incubation study. *J Int Med Res*. 2022;50(6):030006052211051. doi:10.1177/03000605221105163
14. Crocker AD, Munday KA. The effect of the renin-angiotensin system on mucosal water and sodium transfer in everted sacs of rat jejunum. *J Physiol*. 1970;206(2):323-333. doi:10.1113/jphysiol.1970.sp009015
15. Mizuno Y, Yoshimura M, Yasue H, et al. Aldosterone production is activated in failing ventricle in humans. *Circulation*. 2001;103(1):72-77. doi:10.1161/01.CIR.103.1.72

16. Silvestre J-S, Heymes C, Oubénaïssa A, et al. Activation of cardiac aldosterone production in rat myocardial infarction. *Circulation*. 1999;99(20):2694-2701. doi:10.1161/01.CIR.99.20.2694
17. Siragy HM, Xue C. Local renal aldosterone production induces inflammation and matrix formation in kidneys of diabetic rats. *Exp Physiol*. 2008;93(7):817-824. doi:10.1113/expphysiol.2008.042085
18. Rigel DF, Fu F, Beil M, Hu C-W, Liang G, Jeng AY. Pharmacodynamic and pharmacokinetic characterization of the aldosterone synthase inhibitor FAD286 in two rodent models of hyperaldosteronism: comparison with the 11β-hydroxylase inhibitor Metyrapone. *J Pharmacol Exp Ther*. 2010;334(1):232-243. doi:10.1124/jpet.110.167148
19. Hofmann A, Brunssen C, Peitzsch M, et al. The aldosterone synthase inhibitor FAD286 is suitable for lowering aldosterone levels in ZDF rats but not in db/db mice. *Horm Metab Res*. 2017;49(06):466-471. doi:10.1055/s-0043-101821
20. Mohamed DM, Shaqura M, Li X, et al. Aldosterone synthase in peripheral sensory neurons contributes to mechanical hypersensitivity during local inflammation in rats. *Anesthesiology*. 2020;132(4):867-880. doi:10.1097/ALN.0000000000003127
21. Deliyanti D, Miller AG, Tan G, Binger KJ, Samson AL, Wilkinson-Berka JL. Neovascularization is attenuated with aldosterone synthase inhibition in rats with retinopathy. *Hypertension*. 2012;59(3):607-613. doi:10.1161/HYPERTENSIONAHA.111.188136
22. Yamamoto-Furusho JK, Mendivil-Rangel EJ, Fonseca-Camarillo G. Differential expression of occludin in patients with ulcerative colitis and healthy controls. *Inflamm Bowel Dis*. 2012;18(10):E1999. doi:10.1002/ibd.22835
23. Weber CR, Nalle SC, Tretiakova M, Rubin DT, Turner JR. Claudin-1 and claudin-2 expression is elevated in inflammatory bowel disease and may contribute to early neoplastic transformation. *Lab Invest*. 2008;88(10):1110-1120. doi:10.1038/labinvest.2008.78
24. Fries W, Renda MC, Lo Presti MA, et al. Intestinal permeability and genetic determinants in patients, first-degree relatives, and controls in a high-incidence area of Crohn's disease in southern Italy. *Am J Gastroenterol*. 2005;100(12):2730-2736. doi:10.1111/j.1572-0241.2005.00325.x
25. Venkatraman A, Ramakrishna BS, Pulimood AB, Patra S, Murthy S. Increased permeability in dextran Sulphate colitis in rats: time course of development and effect of butyrate. *Scand J Gastroenterol*. 2000;35(10):1053-1059. doi:10.1080/003655200451171
26. Aleksiejczuk M, Gromotowicz-Poplawska A, Marcinczyk N, Stelmaszewska J, Dzieciol J, Chabielska E. Aldosterone increases vascular permeability in rat skin. *Cell*. 2022;11(17):2707. doi:10.3390/cells11172707
27. Kirsch T, Beese M, Wyss K, et al. Aldosterone modulates endothelial permeability and endothelial nitric oxide synthase activity by rearrangement of the actin cytoskeleton. *Hypertension*. 2013;61(2):501-508. doi:10.1161/HYPERTENSIONAHA.111.196832
28. Moretó M, Cristià E, Pérez-Bosque A, Afzal-Ahmed I, Amat C, Naftalin RJ. Aldosterone reduces crypt colon permeability during low-sodium adaptation. *J Membr Biol*. 2005;206(1):43-51. doi:10.1007/s00232-005-0772-5
29. Tveden-Nyborg P, Bergmann TK, Jessen N, Simonsen U, Lykkesfeldt J. BCPT policy for experimental and clinical studies. *Basic Clin Pharmacol Toxicol*. 2021;128(1):4-8. doi:10.1111/bcpt.13492
30. Martin JC, Bériou G, Josien R. Dextran sulfate sodium (DSS)-induced acute colitis in the rat. *Methods Mol Biol*. 2016;197-203. doi:10.1007/978-1-4939-3139-2_12
31. Ménard J, Gonzalez M-F, Guyene T-T, Bissery A. Investigation of aldosterone-synthase inhibition in rats. *J Hypertens*. 2006;24(6):1147-1155. doi:10.1097/01.hjh.0000226205.65442.f2
32. Viennois E, Chen F, Laroui H, Baker MT, Merlin D. Dextran sodium sulfate inhibits the activities of both polymerase and reverse transcriptase: lithium chloride purification, a rapid and efficient technique to purify RNA. *BMC Res Notes*. 2013;6(1):360. doi:10.1186/1756-0500-6-360
33. Yadav VR, Suresh S, Devi K, Yadav S. Effect of Cyclodextrin complexation of curcumin on its solubility and antiangiogenic and anti-inflammatory activity in rat colitis model. *AAPS PharmSciTech*. 2009;10(3):752-762. doi:10.1208/s12249-009-9264-8
34. Melgar S, Karlsson A, Michaëlsson E. Acute colitis induced by dextran sulfate sodium progresses to chronicity in C57BL/6 but not in BALB/c mice: correlation between symptoms and inflammation. *Am J Physiol Liver Physiol*. 2005;288(6):G1328-G1338. doi:10.1152/ajpgi.00467.2004
35. Wirtz S, Popp V, Kindermann M, et al. Chemically induced mouse models of acute and chronic intestinal inflammation. *Nat Protoc*. 2017;12(7):1295-1309. doi:10.1038/nprot.2017.044
36. Vandesompele J, De Preter K, Pattyn F, et al. Accurate normalization of real-time quantitative RT-PCR data by geometric averaging of multiple internal control genes. *Genome Biol*. 2002;3(7) research0034.1–0034.11. doi:10.1186/gb-2002-3-7-research0034
37. Siltari A, Roivanen J, Korpela R, Vapaatalo H. Long-term feeding with bioactive tripeptides in aged hypertensive and normotensive rats: special focus on blood pressure and bradykinin-induced vascular reactivity. *J Physiol Pharmacol*. 2017;68(3):407-418.
38. Gollisch KSC, Brandauer J, Jessen N, et al. Effects of exercise training on subcutaneous and visceral adipose tissue in normal- and high-fat diet-fed rats. *Am J Physiol Metab*. 2009;297(2):E495-E504. doi:10.1152/ajpendo.90424.2008
39. Lee CH, Kim KW, Lee D-H, Lee SM, Kim SY. Overexpression of the receptor for advanced glycation end-products in the auditory cortex of rats with noise-induced hearing loss. *BMC Neurosci*. 2021;22(1):38. doi:10.1186/s12868-021-00642-3
40. Satoh M, Nakamura M, Saitoh H, et al. Aldosterone synthase (CYP11B2) expression and myocardial fibrosis in the failing human heart. *Clin Sci (Lond)*. 2002;102(4):381-386. doi:10.1042/cs1020381
41. Salmenkari H, Issakainen T, Vapaatalo H, Korpela R. Local corticosterone production and angiotensin-I converting enzyme shedding in a mouse model of intestinal inflammation. *World J Gastroenterol*. 2015;21(35):10072-10079. doi:10.3748/wjg.v21.i35.10072
42. Cima I, Corazza N, Dick B, et al. Intestinal epithelial cells synthesize glucocorticoids and regulate T cell activation. *J Exp Med*. 2004;200(12):1635-1646. doi:10.1084/jem.20031958

43. Salmenkari H, Pasanen L, Linden J, Korpela R, Vapaatalo H. Beneficial anti-inflammatory effect of angiotensin-converting enzyme inhibitor and angiotensin receptor blocker in the treatment of dextran sulfate sodium-induced colitis in mice. *J Physiol Pharmacol*. 2018;69(4). doi:10.26402/jpp.2018.4.07
44. Gromotowicz-Poplawska A, Szoka P, Zakrzeska A, et al. Hyperglycemia potentiates prothrombotic effect of aldosterone in a rat arterial thrombosis model. *Cell*. 2021;10(2):471. doi:10.3390/cells10020471
45. Johnson LA, Govani SM, Joyce JC, Waljee AK, Gillespie BW, Higgins PDR. Spironolactone and colitis: increased mortality in rodents and in humans. *Inflamm Bowel Dis*. 2012;18(7):1315-1324. doi:10.1002/ibd.21929
46. Verhamme K, Mosis G, Dieleman J, Stricker B, Sturkenboom M. Spironolactone and risk of upper gastrointestinal events: population based case-control study. *BMJ*. 2006;333(7563):330. doi:10.1136/bmj.38883.479549.2F
47. Pang Z, Korpela R, Vapaatalo H. Intestinal aldosterone synthase activity and aldosterone synthesis in mouse. *J Physiol Pharmacol*. 2022;73(4):503-512. doi:10.26402/jpp.2022.4.03
48. Holloway CD, MacKenzie SM, Fraser R, et al. Effects of genetic variation in the aldosterone synthase (CYP11B2) gene on enzyme function. *Clin Endocrinol (Oxf)*. 2009;70(3):363-371. doi:10.1111/j.1365-2265.2008.03383.x
49. Kupari M, Hautanen A, Lankinen L, et al. Associations between human aldosterone synthase (CYP11B2) gene polymorphisms and left ventricular size, mass, and function. *Circulation*. 1998;97(6):569-575. doi:10.1161/01.CIR.97.6.569
50. Li N, Li J, Ding Y, et al. Novel mutations in the CYP11B2 gene causing aldosterone synthase deficiency. *Mol Med Rep*. 2016;13(4):3127-3132. doi:10.3892/mmr.2016.4906
51. Chassaing B, Aitken JD, Malleshappa M, Vijay-Kumar M. Dextran sulfate sodium (DSS)-induced colitis in mice. *Curr Protoc Immunol*. 2014;104(1):15.25.1-15.25.14. doi:10.1002/0471142735.im1525s104
52. Erben U, Loddenkemper C, Doerfel K, et al. A guide to histomorphological evaluation of intestinal inflammation in mouse models. *Int J Clin Exp Pathol*. 2014;7(8):4557-4576.
53. Altmann GG. Renewal of the intestinal epithelium: new aspects as indicated by recent ultrastructural observations. *J Electron Microsc Tech*. 1990;16(1):2-14. doi:10.1002/jemt.1060160103
54. Nishina H, Katou-Ichikawa C, Kuramochi M, Izawa T, Kuwamura M, Yamate J. Participation of somatic stem cells, recognized by a unique A3 antibody, in mucosal epithelial regeneration in dextran sulfate sodium (DSS)–induced rat colonic lesions. *Toxicol Pathol*. 2020;48(4):560-569. doi:10.1177/0192623320906817
55. Noti M, Corazza N, Mueller C, Berger B, Brunner T. TNF suppresses acute intestinal inflammation by inducing local glucocorticoid synthesis. *J Exp Med*. 2010;207(5):1057-1066. doi:10.1084/jem.20090849
56. Naito Y, Takagi T, Handa O, et al. Enhanced intestinal inflammation induced by dextran sulfate sodium in tumor necrosis factor-alpha deficient mice. *J Gastroenterol Hepatol*. 2003;18(5):560-569. doi:10.1046/j.1440-1746.2003.03034.x
57. Eichele DD, Kharbanda KK. Dextran sodium sulfate colitis murine model: an indispensable tool for advancing our understanding of inflammatory bowel diseases pathogenesis. *World J Gastroenterol*. 2017;23(33):6016-6029. doi:10.3748/wjg.v23.i33.6016
58. Yamagami S, Kawasaki E, Egawa A, et al. Studies on the disposition of Fadrozole hydrochloride (CGS 16949A) (I): absorption, distribution, metabolism and excretion after a single Oral administration to rats. *Drug Metab Pharmacokinet*. 1993;8(5):1097-1127. doi:10.2133/dmpk.8.1097

SUPPORTING INFORMATION

Additional supporting information can be found online in the Supporting Information section at the end of this article.

How to cite this article: Launonen H, Luiskari L, Linden J, et al. Adverse effects of an aldosterone synthase (CYP11B2) inhibitor, fadrozole (FAD286), on inflamed rat colon. *Basic Clin Pharmacol Toxicol*. 2023;133(3):211-225. doi:10.1111/bcpt.13918